

Ain Shams University Faculty of Engineering

DISTORTIONAL BUCKLING OF COLD-FORMED C AND Z MEMBERS IN BENDING

By

TAMER HANAFY SAIED

B.Sc. Civil Engineering (2003) Ain Shams University

A Thesis
Submitted in Partial Fulfillment of the Requirements
Of the Degree of Master of Science in Civil Engineering (Structural)

Under the supervision of:

Prof. Dr. ABDELRAHIM K. DESSOUKI

Professor of Steel Construction and Bridges Structural Engineering Dept. Ain Shams University, Cairo.

Prof. Dr. SHERIF K. HASSAN

Professor of Steel Construction and Bridges Structural Engineering Dept. Ain Shams University, Cairo.

Dr. AHMED H. YOUSEF

Associate Professor Structural Engineering Dept. Ain Shams University, Cairo.

Cairo - 2009

CHAPTER 1

LITERATURE REVIEW

1.1 Introduction

Cold-formed steel members are made from structural steel sheets and formed into shape, either through press-braking blanks sheared from sheets or more commonly, by roll forming the steel through a series of dies. The idea behind cold-formed steel members is to use shapes with higher stiffness rather than thickness to support load. Due to the relatively easy method of manufacturing, a large number of different configurations can be produced to fit the demands of optimized design for both structural and economical purposes. Most commonly, coldformed lipped C and lipped Z-sections have been widely used in light gauge steel construction, as roof purlins or the intermediate members between the main structural frames and the corrugated roof. The use of cold-formed steel members in building construction began at 1850's (Yu 2001). Since the 1940's, cold-formed steel members have been widely used in both industrial and residential buildings. Cold-formed steel represents over 45% of today's steel construction market, and this share is increasing.

For cold-formed flexural members, a mode of buckling intermediate between local and lateral torsional buckling can occur for edge-stiffened C and Z-sections. This mode is known as distortional buckling which involves rotation of the flange lip about the flange-web junction. Figure (1-1) shows the different buckling modes obtained from a finite strip analysis of Z-section conducted by Schafer and Peköz. (1998a).

Three different buckling modes are identified from the finite strip results. The first minimum, at a half-wavelength of 5 in., is the local

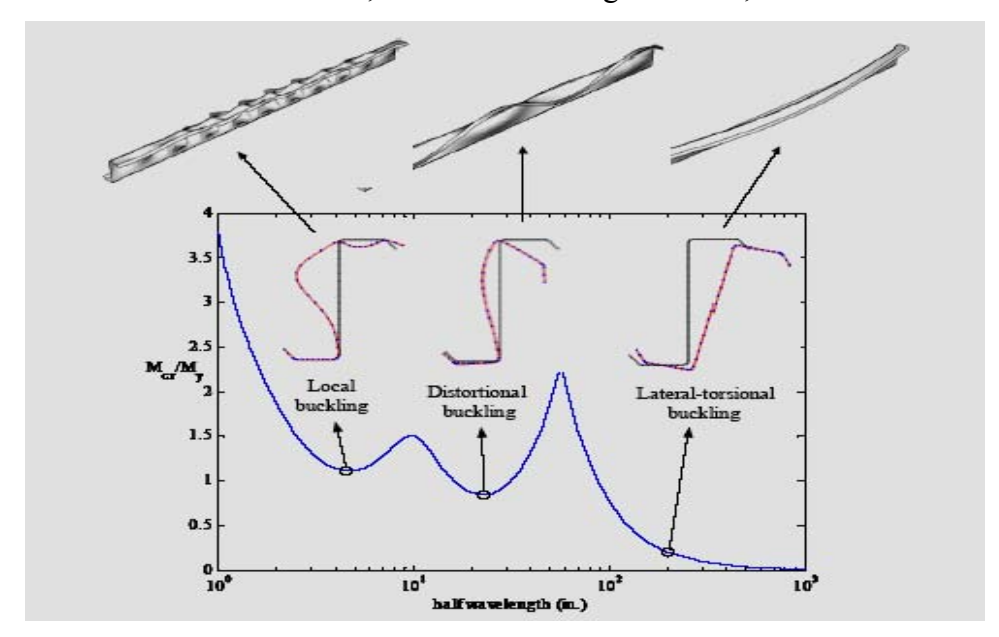


Figure (1-1): Buckling modes of Z-section steel beam (Schafer and Peköz. 1998a)

buckling mode. The distortional buckling mode occurs at the second minimum point of the half-wavelength (at approximately 20 in.). In the distortional mode, the section distorts and the compression flange-lip component rotates about the web-flange junction. In the lateral-torsional mode, the section translates and rotates as a rigid-body without any change in the cross-sectional shape.

Figure (1-2) shows the different buckling modes of C-sections studied by Hancock (1997). Intermediate half-wavelength distortional buckling includes two possible buckling modes, i.e. lip/flange and flange/web, as shown in figure (1-3). Lip/flange distortional buckling mainly involves a rotation of the lip/flange juction about the flange/web corner. However, this buckling mode is influenced by an apparent lateral movement of the flange/web corner, which includes transverse bending

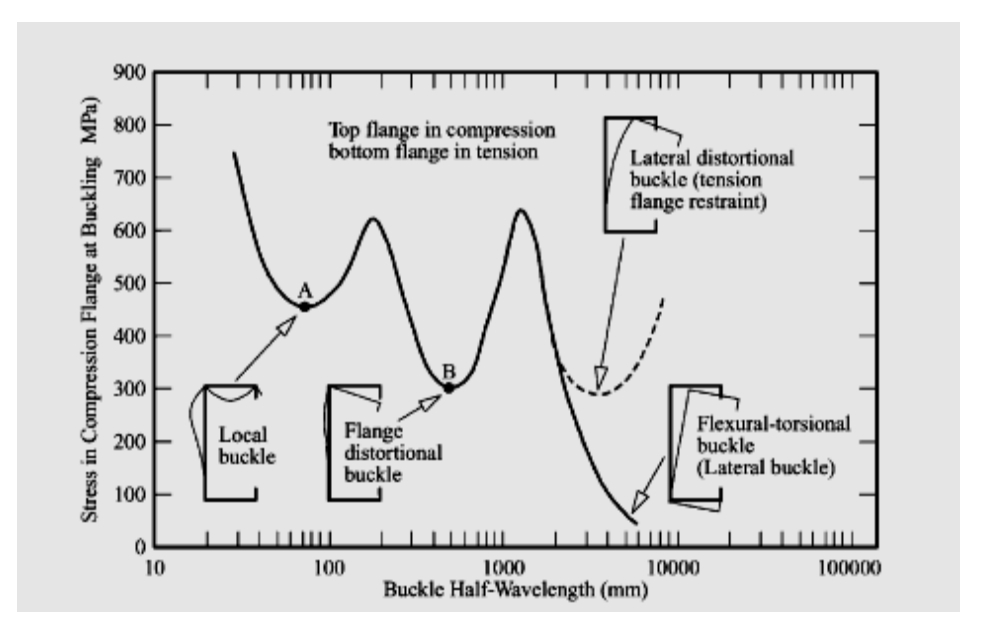


Figure (1-2): Buckling modes of C-section steel beam (Hancock 1997)

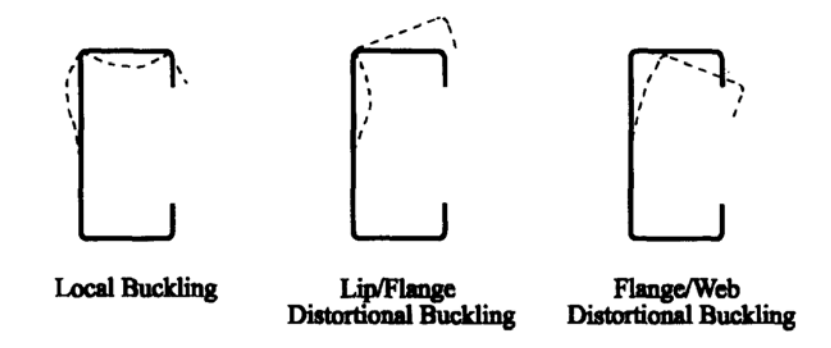


Figure (1-3): Local and short half-wavelength distortional buckling modes

of the web near failure. Both failure modes must be distinguished from the lateral-distortional buckling mode where the lip-flange component, as well as the web, buckle laterally at longer half-wavelengths as shown in Figure (1-2). Flange/web distortional buckling or the lateral-distortional buckling mode often happens when the compression flange is laterally restrained by long interval intermittent bracing.

Distortional buckling most often occurs in sections where lateral deformations (i.e. lateral-torsional buckling) are prevented by intermittent bracing (Ellifritt et al. 1998). Roof purlins are loaded through the cladding members which provide both rotational and translational restraints. These restrains reduce the tendency to lateral-torsional buckling and increase the tendency to local and distortional buckling. Also when the compression flange is not restrained by attachment to sheathing or paneling, such as in the negative bending moments of continuous beams, i.e. joists and purlin, they are prone to distortional failures.

Distortional buckling of cold-formed sections has been recognized to be too complex to be analytically predicted. It is much more complicated than both local and global buckling modes. Distortional buckling is a well-known phenomenon in the literature since 1940s. Approximate analytical methods were developed in the 1960s for predicting distortional buckling stress. In the 1970s, methods based on the finite elements were introduced. It was found that the elastic buckling formulas were not accurate enough in predicting the failure mode. The finite strip method (FSM) was first introduced in the 1980s to calculate distortional buckling stress. FSM can be effectively used in structures that have regular geometry along their length. It also assumes simply supported end boundary conditions and is applicable for longer sections where multiple half-waves occur along the section length.

The progress in distortional buckling studies increased intensevily in the 1990s, when the interaction of distortional buckling with other modes was examined. Various methods were proposed for the distortional buckling analysis of cold-formed steel members.

1.2 Hancock et al. (1996)

An analytical method for the prediction of short half-wavelength distortional buckling and design curves for determining the distortional buckling strength has been presented by Hancock et al. (1996).

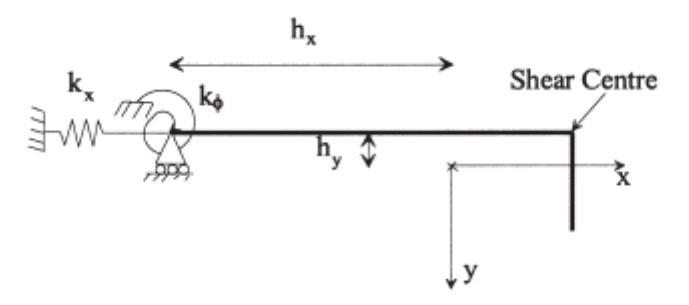


Figure (1-4): Lau and Hancock's model for distortional buckling (1987).

The elastic distortional buckling stress is based on the flexural-torsional buckling of a simple flange, as shown in Figure (1-4). The rotational spring stiffness k_{ϕ} , represents the flexural restraint provided by the web, and the translational spring stiffness k_x , represents the resistance to translational movement of the section in the buckling mode. The model includes a reduction in the flexural restraint provided by the web as a result of the compressive stress distribution in the web element. Lau and Hancock's analysis (1987), demonstrated that the translational spring stiffness k_x does not have much significance and is assumed to be zero. The rotational spring stiffness k_{ϕ} can be expressed as follows:

$$k_{\phi} = \frac{2Et^{3}}{5.46(b_{w} + 0.06\lambda_{d})} \left[1 - \frac{1.11f_{ed}}{Et^{2}} \left(\frac{b_{w}^{4}\lambda_{d}^{2}}{1256\lambda_{d}^{4} + 2.192b_{w}^{4} + 13.39\lambda_{d}^{2}b_{w}^{2}} \right) \right]$$
(1.1)

where $f_{\it ed}$ is the elastic distortional buckling stress of the lip/flange component, and the compressive stress distribution in the web element

computed assuming k_{ϕ} is zero, b_{w} is the web depth, t is the thickness of the section, E is Young's modulus and λ_{d} is then has the form:

$$\lambda_d = 4.80 \left(\frac{I_{xf} b_f^2 b_w}{2t^3} \right)^{0.25} \tag{1.2}$$

The elastic distortional buckling stress then has the form:

$$f_{ed} = \frac{E}{2A_f} \left((\alpha_1 + \alpha_2) \pm \sqrt{(\alpha_1 + \alpha_2)^2 - 4\alpha_3} \right)$$
 (1.3)

where A_f is the cross-sectional area of the flange and stiffener and α_1 , α_2 and α_3 are characteristic values of some complexity which are related to the k_{ϕ} , the half-wavelength in buckling, the geometry and dimensions of the flange and the lip.

The computation process is iterative due to the incorporation of f_{ed} in k_{ϕ} , but only one iteration is required. The method is similar to that of Lau & Hancock (1987) for compression members, but involves modified torsional restraint stiffness, k_{ϕ} at the flange/web corner. The modified torsional restraint stiffness is calculated on the basis of assumed elastic distortional buckling stress, f_{ed} , of the lip/flange component, and the compressive stress distribution in the web element. This method is divided into two models which differ in the formulation of the strength expressions used to determine the inelastic critical buckling stress f_c . These strength curves are based on the column strength expressions for post buckling behavior, as well as the interaction of buckling and yielding.

Strength curve 1:

For
$$f_{ed} > 2.2 f_y$$

$$f_C = f_y \tag{1.4}$$

For $f_{ed} \le 2.2 f_y$

$$f_c = f_y \sqrt{\frac{f_{ed}}{f_y}} \left(1 - 0.22 \sqrt{\frac{f_{ed}}{f_y}} \right)$$
 (1.5)

Strength curve 2:

For
$$f_{ed} > 3.18 f_y$$

$$f_c = f_{v} \tag{1.6}$$

For $f_{ed} \leq 3.18 f_{y}$

$$f_c = f_y \left(\frac{f_{ed}}{f_y}\right)^{0.6} \left(1 - 0.25 \left(\frac{f_{ed}}{f_y}\right)^{0.6}\right)$$
 (1.7)

The full unreduced section modulus is used to calculate the bending moment resistance when the web element torsionally restrains the lip/flange component, i.e. the torsional restraint stiffness, \mathbf{k}_{ϕ} , is greater than or equal to zero. For sections where the lip/flange component torsionally restrains the web element, i.e. the torsional restraint stiffness is less than zero, the effective section modulus is used. When required, effective widths of the lip, flange and web elements are calculated at stress f_c . The effective section modulus is determined with the plate buckling coefficient for the flange set at $\mathbf{k}=4.0$ in the effective width equation. However, local buckling and the assumed stress for the edge stiffener is set at the maximum compression stress in the section f_c .

1.3 Marsh 1990

Another method developed by Marsh (1990) is being considered for adoption by the International Standards Organization for the analysis of the short half-wavelength distortional buckling mode of failure of cold-formed aluminum sections. Modifications were made to ensure that the method is applicable to non-symmetric sections in bending.

A difference exists in the calculation of effective section properties, where a reduced thickness is used for compressive elements instead of the reduced effective width concept. The elastic distortional buckling stress is a function of the geometric properties of the compressive lip/flange component and is determined in accordance with the strength expressions specified in the current S136-94, Cold Formed Steel Structure Members, Canadian Standards Association. An overall normalized section slenderness is calculated and compared with the normalized slenderness of the compressive lip, flange and web elements. Elements which have a normalized slenderness greater than that of the overall section are reduced in thickness. The overall section slenderness λ and normalized overall section slenderness $\overline{\lambda}$ are given as follows:

$$\lambda = \pi \left(\frac{EI_p}{GJ \ 2(EC_w k_\phi)^{1/2}} \right)^{1/2}$$
 (1.8)

$$\overline{\lambda} = \frac{\lambda}{\pi} \sqrt{\frac{f_c}{E}} \tag{1.9}$$

Where f_c is the maximum compressive stress in the section, e.g. f_y , I_p is the polar moment of inertia of the lip/flange component about the flange/web corner, and C_w and J are the warping constant and torsion constant of the lip/flange component, respectively. The normalized inelastic critical buckling stress, f_{ed} , is calculated as follows:

For
$$\overline{\lambda} \le \sqrt{2}$$

$$f_{ed} = f_c (1 - \overline{\lambda}^2) / 4 \tag{1.10}$$

For
$$\overline{\lambda} > \sqrt{2}$$

$$f_{ed} = f_c \sqrt{\overline{\lambda}^2}$$

$$f_{ed} \leq f_y$$
(1.11)

The slenderness and normalized slenderness of the compressive flange element is then calculated :

$$\lambda_f = mb_f / t \tag{1.12}$$

$$\overline{\lambda}_f = \frac{\lambda_f}{\pi} \sqrt{\frac{f}{E}} \tag{1.13}$$

where m = 1.6 for flanges supported by a simple edge stiffener If $\overline{\lambda}_f > \overline{\lambda}$ then the reduced thickness of the compressive flange, t_f' is used to calculate the effective section modulus:

$$t_f^t = t \sqrt{\overline{f}_f} \tag{1.14}$$

For
$$\overline{\lambda_f} \le \sqrt{2}$$

$$\overline{f_f} = (1 - \overline{\lambda_f}^2 / 4) \tag{1.15}$$

For
$$\overline{\lambda_f} > \sqrt{2}$$

$$\overline{f_f} = 1/\overline{\lambda_f}^2 \tag{1.16}$$

1.4 Schafer and Peköz (1999)

New procedures for hand prediction of the buckling stress in local and distortional mode were presented and verified by Schafer and Peköz (1999). Since distortional buckling mainly involves the rotation of the flange, the distortional buckling of an entire section can be obtained by considering the lateral-torsional buckling of the compression flange. As shown in Figure (1-5), the flange is modeled as an undistorted column with springs along one edge. The three springs represent the effect of the web.

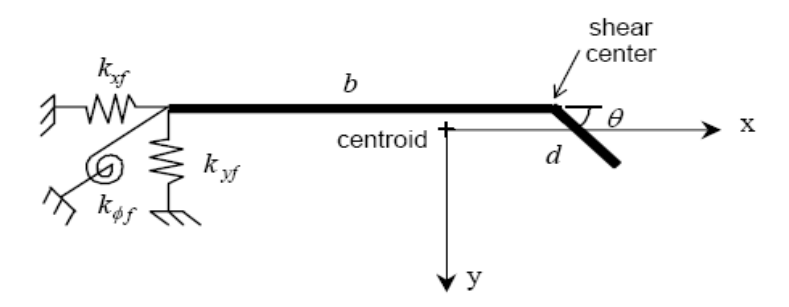


Figure (1-5): Analytical model for flange (Schafer and Peköz 1999)

The work by Schafer and Peköz (1999) proposed an explicit treatment of the role of the elastic and geometric rotational stiffness at the web-flange junction and the method can account for the cases where the buckling is initiated by web instability. The elastic distortional buckling solutions of Schafer and Peköz (1999) are summarized here.

The elastic distortional buckling stress ($f_{\it ed}$) is given as:

$$f_{ed} = \frac{K_{\phi fe} + K_{\phi we}}{\widetilde{K}_{\phi fg} + \widetilde{K}_{\phi wg}}$$
(1.17)

Where $K_{\phi\!f\!e}$ and $K_{\phi\!w\!e}$ are the elastic rotational stiffness of the flange and web, respectively and $\widetilde{K}_{\phi\!f\!g}$ and $\widetilde{K}_{\phi\!w\!g}$ are the stress dependent geometric stiffness of the flange and web, (divided by stress f_{ed}) respectively.

In their work, the Numerical investigations were employed to highlight post-buckling behavior unique to the distortional mode. Local mode is compared to the distortional mode and it was shown that distortion has highlighted imperfection sensitivity, lower buckling capacity and the ability to control failure mechanism even when the elastic local buckling stress is lower than the distortional buckling stress. Comparison with experimental tests shows that the new approach was more reliable than the existing design methods.

1.5 Yu and Schafer (2005)

Existing tests on C and Z-sections generally focus on the performance of the compression flange and do not provide definitive evaluations of the design expressions for the web due to incomplete restriction of the distortional mode and a general lack of information on bracing details. Therefore, experiments were developed by Yu and Schafer (2005) to evaluate the design specifications as well as to examine the Direct Strength Method specifically for distortional buckling of CFS beams. Two series of flexural members, local and distortional buckling, were

tested in order to explore the post-buckling behavior and ultimate strength of cold-formed steel beams. The first test series was local buckling failure mode in which the bracing were considered to ensure restriction of distortion and lateral-torsional buckling.

A series of four-point bending tests is proposed for the local buckling tests. As shown in Figure (1-6) and Figure (1-7), the 16 ft.(4877mm) span length, four-point bending test, consists of a pair of 18 ft. long C or Z-sections in parallel, loaded at the 1/3 points. The members are oriented in an opposed fashion; such that in-plane rotation of the C or Z sections leads to tension in the panel, and thus provides additional restriction against distortional buckling of the compression flange. Small angles $(1\frac{1}{4} \times 1\frac{1}{4} \times 0.057 \text{ in.})$ (32 x 32 x 1.45 mm), are attached (screwed) to the tension flanges every 12 in.(305mm), and a throughfastened standard steel decking (t = 0.019 in.(0.5mm), 1.25 in.(3.2mm) high ribs), is attached (also screwed) to the compression flange.

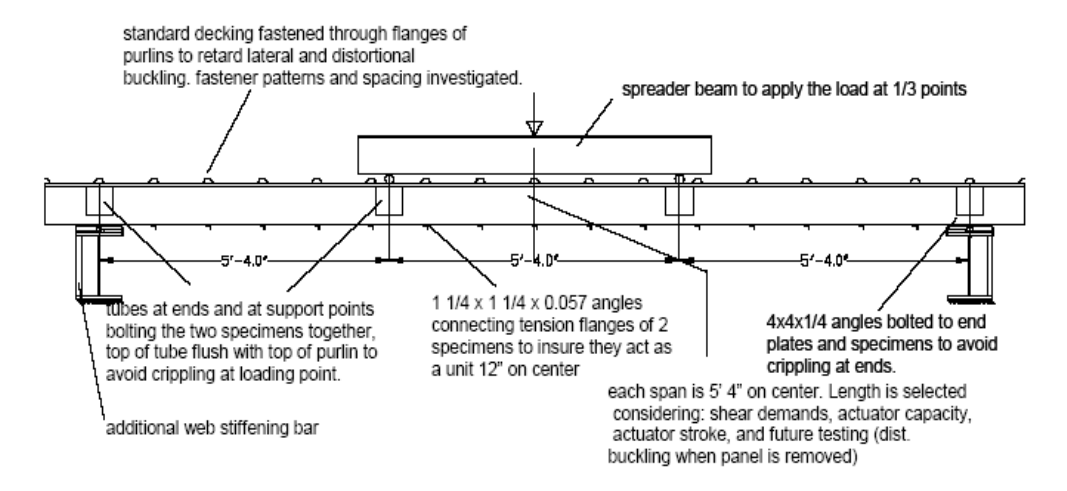


Figure (1-6): Elevation view of overall test arrangement for four point bending test (Yu and Schafer 2005)



Figure (1-7): Overall view of test setup (Yu and Schafer 2005)

The panel-to-section fastener details need to be set carefully to restrict the distortional mode while allowing local bucking to occur and thus trigger the desired failure mode. One way to restrict the distortional buckling mode is to limit the rotation of the compression flange. Figure (1-8) shows the results of a finite strip analysis of a Z-section. When a rotational spring (represented by a star in the figure) is added to the compression flange, the buckling curve moves from curve 1 to curve 2. The elastic distortional buckling moment is increased significantly, but local buckling does not change. In the tests, the standard panel screwed down to the compression flange is expected to work as a rotational spring to restrict the distortional buckling mode.

A pair of fasteners placed on either side of the raised ribs (panel type C as shown in figure) would force local buckling to be the lowest mode. Testing confirmed this prediction, and paired fasteners as shown in figures (1-8) and (1-9) provided a capacity 10% greater than single fasteners and 98% of the AISI (1996) prediction.

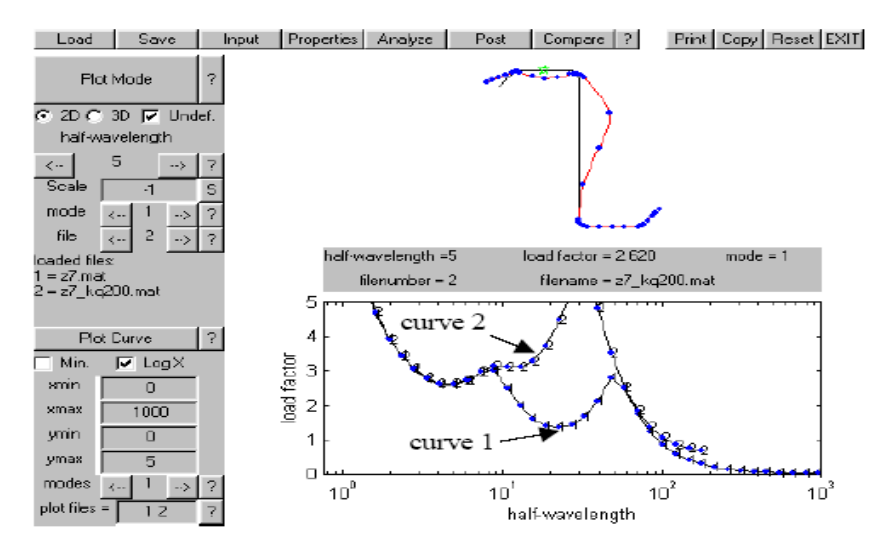


Figure (1-8): Finite strip analysis of Z-section (Yu and Schafer 2005)

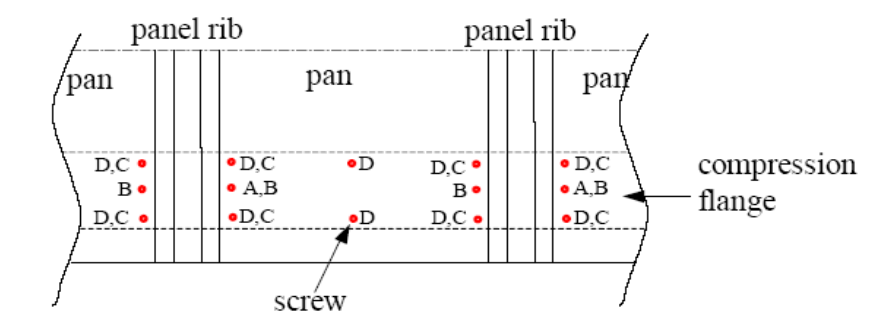


Figure (1-9): Plan view of fastener location for panel to section connection (Yu and Schafer 2005)

Test results indicated that the design methods, such as AISI (1996), AISI (2001), AS/NZS 4600 (1996), EN1993 (2002) and DSM (2004), provide adequate strength predictions in local buckling failures. However, this overall agreement is primarily due to conservative predictions in stocky members that had observable inelastic reserve capacity ($M_{\text{test}}/M_{\text{y}} > 1$).